the plant journal

SEB Society for Experimental Biology

The Plant Journal (2013) **74,** 730–745 doi: 10.1111/tpj.12159

Arabidopsis transcription factor WRKY8 functions antagonistically with its interacting partner VQ9 to modulate salinity stress tolerance

Yanru Hu[1,2], Ligang Chen[1], Houping Wang[1,2], Liping Zhang[1], Fang Wang[1] and Diqiu Yu[1,*]

[1]*Key Laboratory of Tropical Forest Ecology, Xishuangbanna Tropical Botanical Garden, Chinese Academy of Sciences, Kunming, Yunnan 650223, China, and*

[2]*University of Chinese Academy of Sciences, Beijing 100049, China*

Received 29 October 2012; revised 22 January 2013; accepted 21 February 2013; published online 2 March 2013.

*For Correspondence (e-mail ydq@xtbg.ac.cn).

SUMMARY

The WRKY transcription factors have been demonstrated to play crucial roles in regulating stress responses; however, the exact mechanisms underlying their involvement in stress responses are not fully understood. Arabidopsis *WRKY8* was predominantly expressed in roots and was highly upregulated by salt treatment. Disruption of WRKY8 rendered plants hypersensitive to salt, showing delayed germination, inhibited post-germination development and accelerated chlorosis. Further investigation revealed that WRKY8 interacted with VQ9, and their interaction decreased the DNA-binding activity of WRKY8. The VQ9 protein was exclusively localized in the nucleus, and *VQ9* expression was strongly responsive to NaCl treatment. Mutation of *VQ9* enhanced tolerance to salt stress, indicating that VQ9 acts antagonistically with WRKY8 to mediate responses to salt stress. The antagonist functions of WRKY8 and VQ9 were consistent with an increased or reduced Na^+/K^+ concentration ratio, as well as contrasting expression patterns of downstream stress-responsive genes in salt-stressed *wrky8* and *vq9* mutants. Moreover, chromatin immunoprecipitation (ChIP) assays showed that WRKY8 directly bound the promoter of *RD29A* under salt conditions. These results provided strong evidence that the VQ9 protein acts as a repressor of the WRKY8 factor to maintain an appropriate balance of WRKY8-mediated signaling pathways to establish salinity stress tolerance.

Keywords: WRKY8, VQ9, salt stress, ion homeostasis, *RD29A*, Arabidopsis.

INTRODUCTION

In nature, plants are challenged with various environmental stresses, such as extreme temperatures, low water availability and soils with changing salt or nutrient concentrations. These abiotic stresses are the main causes of crop failure worldwide, reducing average yields of major crop plants by more than 50% (Bray *et al.*, 2000). Soil salinity is one of the most serious threats for world agriculture, and is becoming particularly widespread in many regions (Wang *et al.*, 2003). High salinity imposes osmotic, ionic and secondary oxidative stresses upon plant cells, and ultimately affects plant growth and development (Zhu, 2001).

To tolerate salt stress, plants have evolved sophisticated mechanisms involving altered physiological, morphological and biochemical processes (Zhu, 2002; Wang *et al.*, 2003; Tuteja, 2007; Munns and Tester, 2008; Zhang *et al.*, 2012). In Arabidopsis, these salt tolerance mechanisms include the restoration of ion balance in the cell, accumulation of antioxidant enzymes, synthesis of compatible 'products, alterations to gene expression and a reduction in growth rate (Zhu, 2002; Munns and Tester, 2008; Zhang *et al.*, 2012). For example, under salt stress conditions, ion homeostasis is stringently regulated so that essential ions accumulate while toxic ions remain low (Zhu, 2003; Cheong and Yun, 2007). Previous studies have revealed that the SOS (for Salt Overly Sensitive) pathway plays critical roles in regulating ion homeostasis to confer salt tolerance (Qiu *et al.*, 2004; Mahajan *et al.*, 2008).

The WRKY family of transcription factors is defined by the presence of a conserved WRKYGQK amino acid sequence, and can be subdivided into three groups (Eulgem *et al.*, 2000; Rushton *et al.*, 2010). Many studies have demonstrated that WRKY factors play crucial roles in regulating defense responses (Pandey and Somssich, 2009). For example, disruption of the structurally related WRKY11 or WRKY17 resulted in enhanced resistance to the biotrophic pathogen *Pseudomonas syringae* (Journot-Catalino

© 2013 The Authors
The Plant Journal © 2013 John Wiley & Sons Ltd

et al., 2006). In addition, mutations in *WRKY33* increased susceptibility to the necrotrophic fungal pathogen *Botrytis cinerea* (Zheng *et al.*, 2006). Besides defense responses, WRKY proteins also participate in regulating certain abiotic stress responses (Chen *et al.*, 2012). Our previous reports showed that WRKY25, WRKY26 and WRKY33 coordinate the induction of plant thermotolerance (Li *et al.*, 2011). Moreover, the structurally related proteins WRKY6 and WRKY42 were reported to play a role in low-phosphate stress responses (Chen *et al.*, 2009).

The WRKY proteins specifically recognize the W-box elements containing a TGAC core sequence in downstream target-gene promoters during stress responses. For example, a recent study demonstrated direct *in vivo* interactions between WRKY40 and the promoter regions of several defense-related genes (Pandey *et al.*, 2010). Very recently, WRKY33 was shown to directly regulate the expressions of several critical components of defense-signaling pathways during *B. cinerea* infection (Birkenbihl *et al.*, 2012; Li *et al.*, 2012). Thus, members of the WRKY family may function as crucial regulators of stress signaling to establish appropriate resistance or tolerance; however, the regulatory mechanisms of the involvement of WRKY factors in stress responses are still not fully understood.

Previously, we demonstrated the importance of the transcription factor WRKY8 in basal resistance against pathogen infections (Chen *et al.*, 2010a). Here, we report the role of WRKY8 in mediating salt stress tolerance. The *WRKY8* gene was predominantly expressed in roots and was highly upregulated by NaCl treatment. Phenotype analyses indicated that the WRKY8 transcription factor acts as a positive regulator of salt stress. Further investigation showed that WRKY8 interacted in the nucleus with VQ9, a VQ motif-containing protein. Experimental results suggested that VQ9 decreased the DNA binding activity of WRKY8, thereby negatively regulating salinity stress responses. The functional antagonism between WRKY8 and VQ9 may be a specific mechanism to maintain an appropriate balance of WRKY8-mediated signaling pathways to establish salt tress tolerance.

RESULTS

Expression analyses of WRKY8

In a previous study, we showed that *WRKY8* is induced by pathogen attack and is involved in defense responses. To further clarify the potential functions of *WRKY8*, we examined its expression profiles more precisely. First, we examined the basic expression of *WRKY8* by quantitative real-time PCR (qRT-PCR). As shown in Figure 1(a), we detected high levels of *WRKY8* transcripts in roots and low levels in rosette leaves and siliques. *WRKY8* transcripts were barely detected in cauline leaves, stems and flowers. We also measured the induced expression of *WRKY8* in response to certain abiotic stresses. *WRKY8* expression was strongly upregulated by high-salinity treatment, but not by other abiotic stresses, including osmotic stress, dehydration, cold and heat (Figure 1b). Together, these results indicated that the *WRKY8* gene mainly responds to salt treatment and may be involved in responses to salinity stress.

Mutation of WRKY8 renders plants hypersensitive to salt

To clarify the role of *WRKY8* in salinity stress responses, we first compared the germination rate between the *wrky8* mutant and the wild type on NaCl-containing medium. We used two previously described *wrky8* mutants (*wrky8-1* and *wrky8-3*) for these analyses (Chen *et al.*, 2010a). Under normal conditions, there was no significant difference in germination between the mutant and the wild type. We then germinated seeds of *wrky8* mutants and wild type on MS agar medium supplemented with various concentrations of NaCl. The germination rate was calculated based on radicle emergence. As shown in Figure 2(a), the germination of *wrky8* seeds was inhibited by salt, compared with that of the wild type. On the high-salt media (175 or 200 mM NaCl), the germination of *wrky8* seeds was inhibited to a greater extent than that of wild-type seeds. These observations indicated that *wrky8* mutants are more sensitive to salt than the wild type during germination, suggesting that WRKY8 may function as a positive regulator of salt stress tolerance.

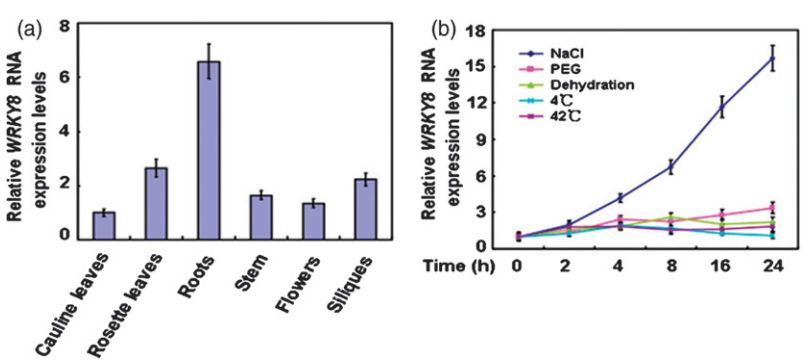

Figure 1. Analyses of *WRKY8* expression.
(a) qRT-PCR analyses of *WRKY8* basal expression. RNA samples were isolated from roots, rosette leaves, cauline leaves, stem, flowers and siliques of wild-type plants grown at 22°C.
(b) qRT-PCR analyses of *WRKY8* expression responding to abiotic stresses. RNA samples were prepared from 3-week-old wild-type plants at the given times after treatment with salt (250 mM NaCl), 25% PEG, cold (4°C) or heat (42°C). Error bars show standard deviations from three independent RNA extractions.

© 2013 The Authors

Next, we evaluated the performance of *wrky8* mutants and wild-type seedlings during post-germination development and vegetative growth stages. As shown in Figure 2(b) and (c), the cotyledon greening of *wrky8* mutants was more vulnerable to NaCl stress compared with the wild type. The cotyledons of most *wrky8* seedlings

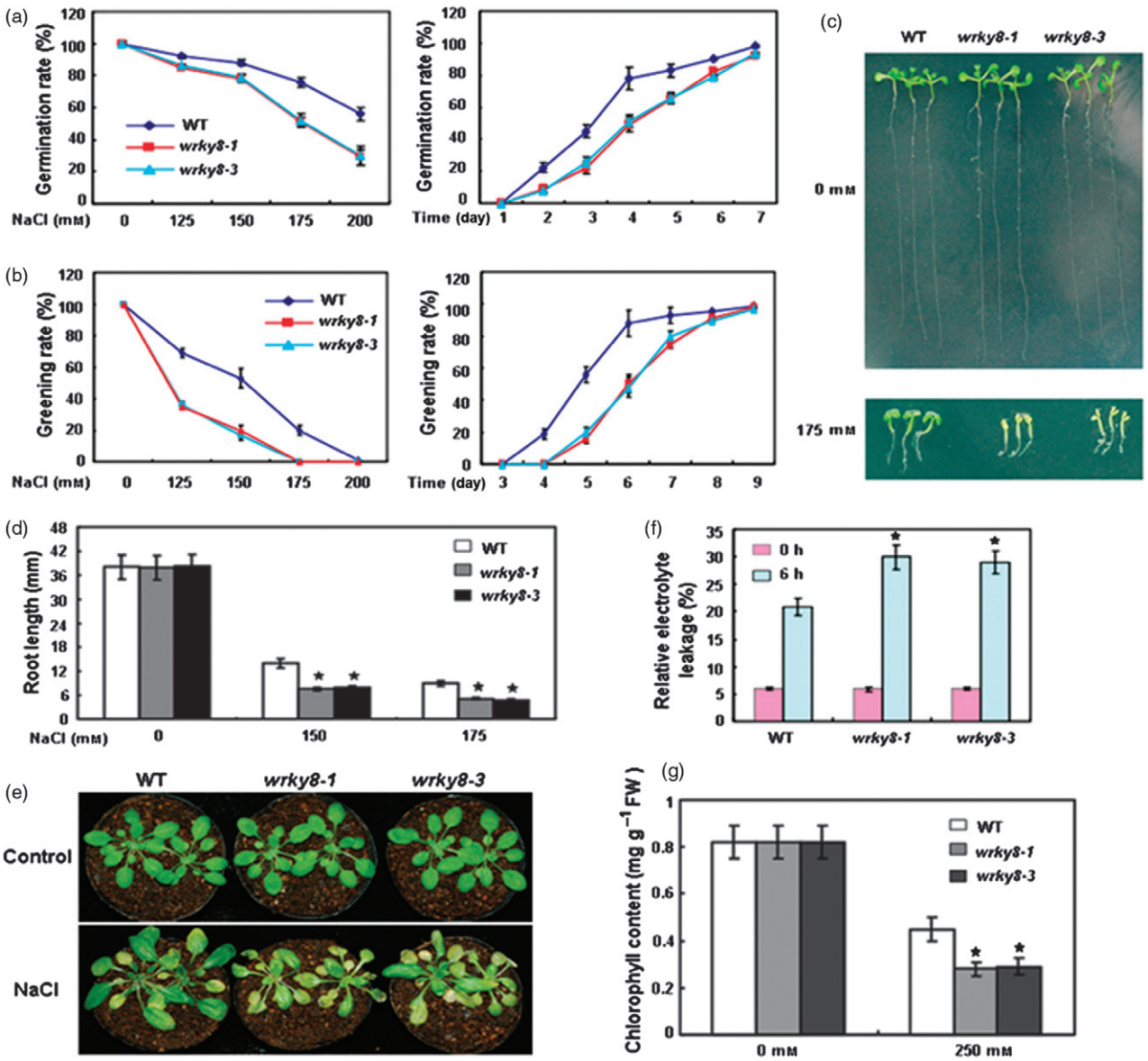

Figure 2. Phenotypic characterization of the *wrky8* mutants.
(a) Seed germination analyses: the germination of wild-type (WT) and *wrky8* mutant seeds on day 4 after stratification on medium supplemented with different concentrations of NaCl (left), and the germination of WT and *wrky8* mutant seeds on 175 mM NaCl medium over 7 days (right). All experiments were performed three times each, evaluating more than 60 seeds; values are means ± SEs.
(b) Cotyledon greening analyses: cotyledon greening rates were scored on day 5 after stratification on medium containing NaCl (left). The greening of WT and *wrky8* mutants on 150 mM NaCl medium over 9 days (right). All experiments were performed in triplicate, each evaluating more than 60 seeds; values are means ± SEs.
(c) Early seedling development analyses: WT and *wrky8* mutant seeds were geminated in MS medium, and 3 days after stratification all were transferred to NaCl-containing medium in a vertical manner. The pictures of representative seedlings were taken 7 days after transfer.
(d) Root elongation analyses. Experiments were performed three times; values are means ± SEs.
(e) Salt-sensitivity analyses of soil-grown *wrky8* mutants: after 3 weeks of growth in soil, the plants were watered with 250 mM NaCl for 18 days and photographed. Control plants were photographed before salt treatments. Experiments were repeated twice using over 50 plants per treatment.
(f) Relative electrolyte leakage analyses: 3-week-old plants were treated with 250 mM NaCl for 6 h; values shown are means ± SEs from three independent experiments.
(g) Chlorophyll contents analyses: the 3-week-old soil-grown plants were watered with 250 mM NaCl for 2 weeks and their chlorophyll contents were then measured. Experiments were repeated three times; values are means ± SEs. *Significant difference between mutant and WT ($P < 0.05$).

© 2013 The Authors

did not expand and were yellow in the presence of 175 mM NaCl, even 10 days after germination in the light (Figure 2c). In addition, the root length of *wrky8* seedlings was more sensitive to salt than that of the wild-type seedlings (Figure 2d). Furthermore, the soil-grown *wrky8* mutants were also more sensitive to salt stress than the wild-type plants, displaying reductions in growth, elevated relative electrolyte leakage and accelerated chlorosis (Figure 2e–g). To further determine the biological roles of WRKY8 in salinity stress responses, we analyzed the performances of *WRKY8* overexpression transgenic plants (*W8*OE) under salt stress. *W8*OE plants were obtained and as previously described by Chen *et al.* (2010a). As shown in Figure 3, constitutive overexpression of *WRKY8* enhanced the tolerance of transgenic plants to salt stress. Taken together, these results further supported the idea that WRKY8 has positive regulatory roles in salt stress responses.

WRKY8 interacts with VQ9 in the nucleus of plant cells

As WRKY8 is involved in salt stress responses, we investigated whether it interacts with partner proteins to mediate salt-stress signaling pathways. The Gal4 transcription activation-based yeast two-hybrid system was used. The *WRKY8* full-length cDNA with a deleted activation domain was fused to the Gal4 DNA-binding domain of the bait vector (BD-WRKY8). After screening, three independent clones

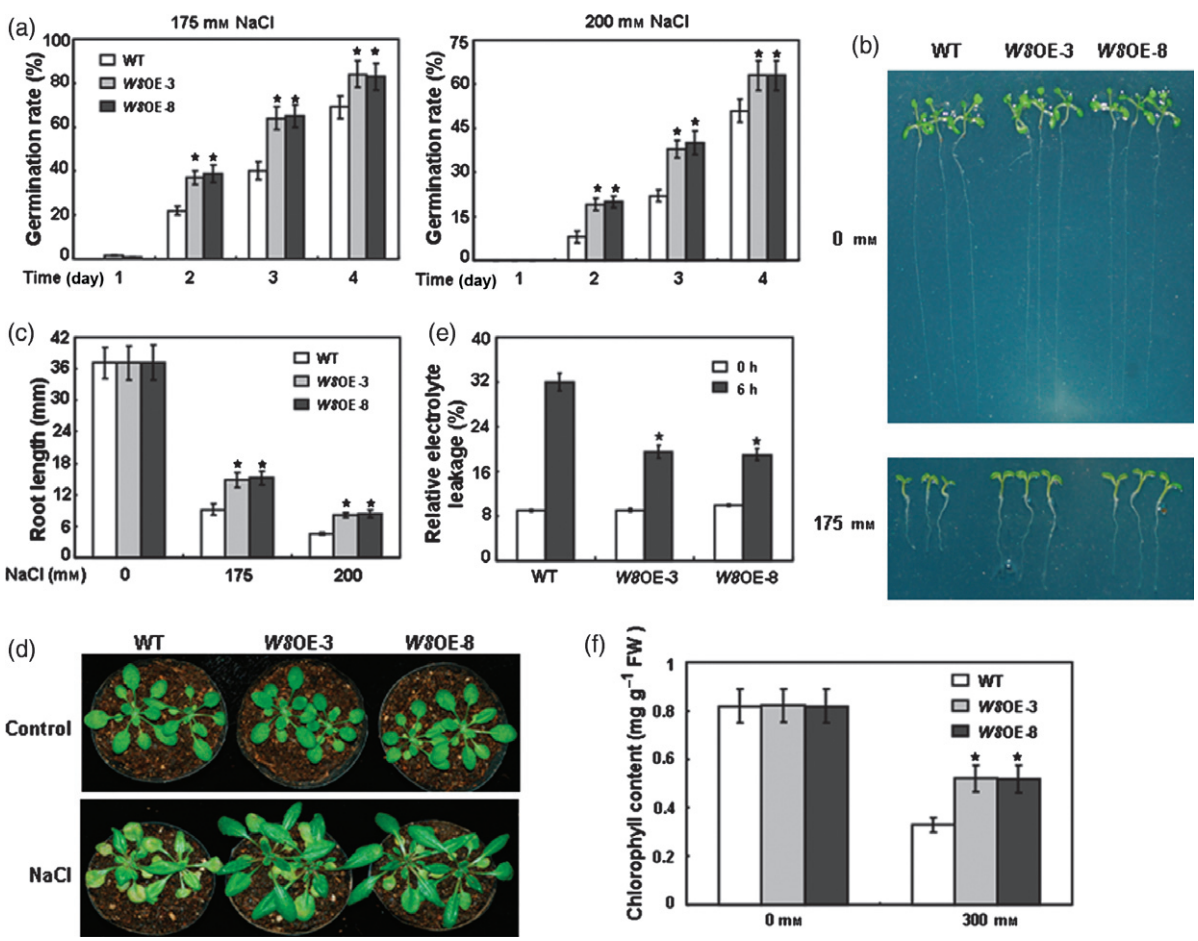

Figure 3. Phenotypic characterization of the *WRKY8* overexpression plants.
(a) Seed germination analyses: all experiments were performed three times, each evaluating more than 60 seeds; values are means ± SEs.
(b) Early seedling development analyses: wild-type (WT) and *WRKY8* overexpression lines were geminated in MS medium, and 3 days after stratification all were transferred to NaCl-containing medium in a vertical manner. Pictures of representative seedlings were taken 7 days after transfer.
(c) Root elongation analyses. Experiments were performed three times; values are means ± SE.
(d) Salt-sensitivity analyses of soil-grown *WRKY8* overexpression plants. After 3 weeks of growth in soil, the plants were watered with 300 mM NaCl for 18 days and photographed. Control plants were photographed before salt treatments. Experiments were repeated twice using over 50 plants per treatment.
(e) Relative electrolyte leakage analyses: 3-week-old plants were treated with 250 mM NaCl for 6 h; values shown are means ± SEs from three independent experiments.
(f) Chlorophyll contents analyses: 3-week-old soil-grown plants were watered with 300 mM NaCl for 2 weeks and their chlorophyll contents were measured. Experiments were repeated three times; values are means ± SEs. *W8*OE, *WRKY8* overexpression plants. *Significant difference between mutant and wild type ($P < 0.05$).

© 2013 The Authors

encoding VQ9 were identified by prototrophy for His and Ade. To confirm the interaction, the full-length *VQ9* cDNA was cloned and introduced into the prey vector (AD-VQ9). The BD-WRKY8 and AD-VQ9 plasmids were co-transformed into yeast and the interaction was reconstructed (Figure 4a). VQ9, containing 311 amino acid residues, is a member of the VQ-motif protein family (Cheng *et al.*, 2012). To confirm whether WRKY8 specifically interacts with VQ9 or not, we also analyzed its interaction with another VQ-motif protein, VQ27. As shown in Figure 4(a), WRKY8 did not interact with VQ27, indicating the specificity of the WRKY8–VQ9 interaction.

To further corroborate that VQ9 interacts with WRKY8, we examined their interaction in plant cells by bimolecular fluorescence complementation (BiFC) and coimmunoprecipitation (CoIP) assays. For the BiFC assays, WRKY8 was fused to the C-terminal yellow fluorescent protein (YFP) fragment (WRKY8-C-YFP) and VQ9 to the N-terminal YFP fragment (VQ9-N-YFP). When fused, WRKY8-C-YFP was co-expressed with VQ9-N-YFP in leaves of *Nicotiana benthamiana* (tobacco), and the YFP signal was detected in the nuclear compartment of transformed cells, as revealed by staining with 4′,6-diamidino-2-phenylindole (DAPI) (Figures 4b and S1a). We did not detect any fluorescence in the negative controls (Figures 4b and S1a). In addition, when WRKY8-C-YFP was co-expressed with VQ27-N-YFP, no fluorescence was observed (Figures 4b and S1a). As well as BiFC assays, the WRKY8–VQ9 interaction was verified by CoIP assays using plant total protein (Figure 4c). These experimental results indicated that WRKY8 forms a protein complex with VQ9 in the nucleus of plant cells.

To further specify the regions of WRKY8 required for the interaction with VQ9, several truncated WRKY8 variants were fused to the Gal4 DNA-binding domain. As shown in Figure S2a, the middle region of WRKY8 (145 amino acids, from position 100 to 244, spanning the WRKY domain and zinc-finger motif) was essential for the interaction with VQ9, as the truncated WRKY8 variants with further deletions of amino acids from position 100 to 188 or with a site-mutated WRKY domain or zinc-finger motif failed to interact with VQ9. To identify the regions of VQ9 responsible for their interaction, we also performed directed yeast two-hybrid analyses. As shown in Figure S2b, deletion of the N terminus (amino acids 1–150, including the VQ motif) of VQ9 completely abolished the WRKY8–VQ9 interaction. To clarify whether the short VQ motif was required for the interaction, we generated a mutant VQ9 ($VQ9^{\Delta VQ\ motif}$) in which the conserved VVQK residues in the VQ motif were replaced by EDLE. The yeast two-hybrid assay showed that there was no interaction in yeast cells harboring both the mutant $VQ9^{\Delta VQ\ motif}$ prey and WRKY8 bait vectors (Figure S2b), suggesting that the VQ motif of VQ9 is critical for the WRKY8–VQ9 interaction.

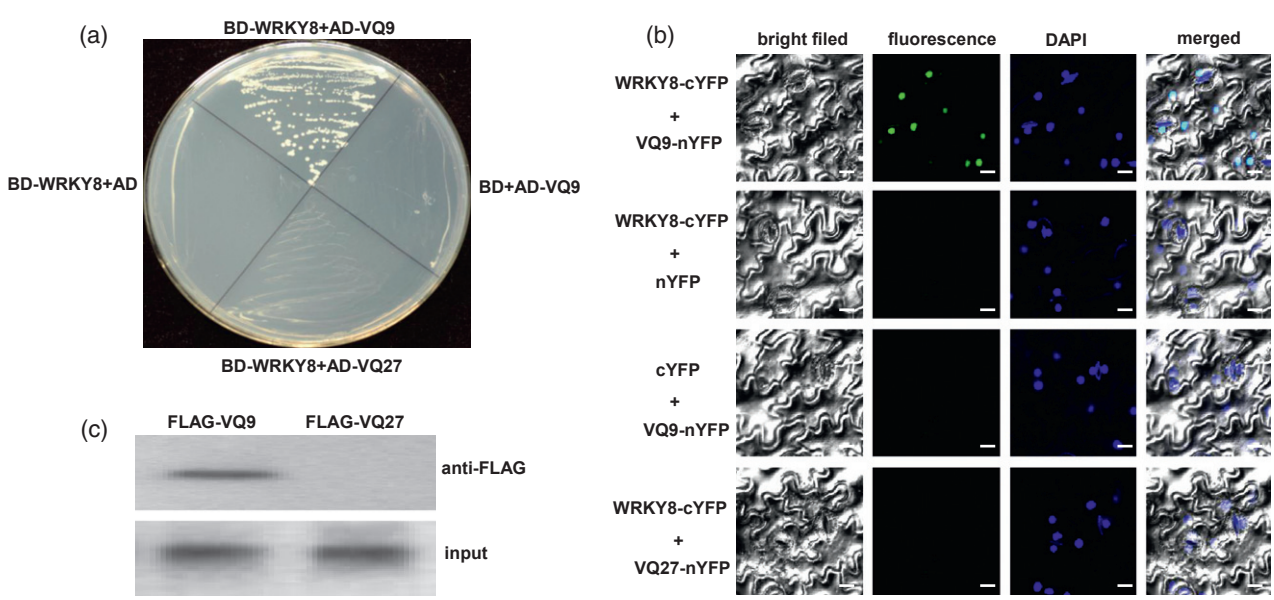

Figure 4. Physical interaction between WRKY8 and VQ9.
(a) Yeast two-hybrid assay analyses. An interaction was indicated by the ability of cells to grow on synthetic drop-out medium lacking Leu, Trp, His and Ade, and containing 15 mM 3-aminotriazole (3-AT).
(b) BiFC analyses. Fluorescence was observed in the nuclear compartment of *N. benthamiana* leaf epidermal cells, which resulted from complementation of the C-terminal part of YFP fused with WRKY8 (WRKY8-C-YFP), with the N-terminal part of YFP fused with VQ9 (VQ9-N-YFP). Scale bars: 10 μm.
(c) CoIP analyses. MYC-fused WRKY8 was immunoprecipitated using anti-MYC antibody and co-immunoprecipitated VQ9 was then detected using an anti-FLAG rabbit antibody. Protein input for MYC-WRKY8 in immunoprecipitated complexes was also detected and shown.

© 2013 The Authors

VQ9 is localized in the nucleus and strongly responds to salinity stress

Because VQ9 physically interacts with WRKY8, we analyzed its properties in more detail. First, we determined its subcellular localization by fusing the full-length VQ9 to green fluorescent protein (GFP) and transiently expressing the construct in leaves of tobacco. As shown in Figures 5(a) and S1b, the transiently expressed VQ9-GFP fusion protein was exclusively localized in the nucleus, as revealed by DAPI staining. In the control, free GFP was found in both the nucleus and the cytoplasm (Figures 5a and S1b). These results indicated that VQ9 is a nuclear protein, consistent with its ability to interact with WRKY8 *in vivo*. As the VQ motif of VQ9 is important for the WRKY8–VQ9 interaction, the VQ9$^{\Delta VQ\ motif}$ construct was also fused to GFP and expressed in leaves of tobacco. Interestingly, the VQ9$^{\Delta VQ\ motif}$ construct displayed fluorescence in both the nucleus and the cytoplasm, sharing the same distribution as the smaller GFP (Figures 5a and S1b).

Next, we examined the expression profiles of *VQ9*. As shown in Figure 5(b), *VQ9* was expressed at higher levels in roots than in other organs under normal growth conditions. We also examined the expression of *VQ9* in response to abiotic stresses. *VQ9* was strongly induced by NaCl treatment and moderately induced by dehydration, but its expression was not induced by heat and cold (Figure 5c). To examine the expression profiles of *VQ9* more precisely, we also measured its expression in response to biotic stresses. As shown in Figure 5(d), *VQ9* transcripts did not change after infection with the biotrophic pathogen *P. syringae* or the necrotrophic pathogen *B. cinerea.* Thus, *VQ9* was mainly expressed in roots and was strongly responsive to salinity stress, sharing similar spatial and temporal expression patterns with *WRKY8*.

VQ9 decreases the DNA-binding activity of WRKY8

WRKY proteins have been shown to specifically bind the W-box sequences through the WRKY domain. As VQ9 interacted with the WRKY8 fragment that overlapped with its DNA-binding domain, we anticipated that the physical interaction may interfere with the DNA-binding activity of

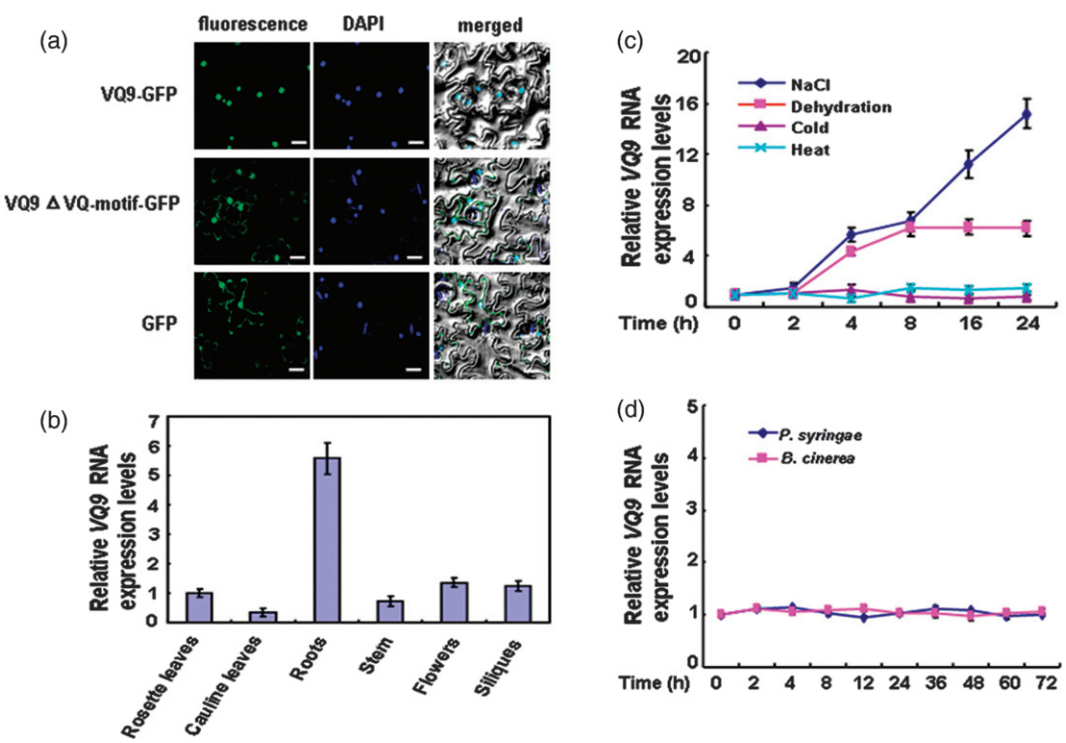

Figure 5. Subcellular localization and expression patterns of VQ9.
(a) Subcellular localization of VQ9: full-length VQ9 protein was exclusively localized in the nucleus, whereas VQ9$^{\Delta VQ\ motif}$ and free GFP were detected in both the nucleus and the cytoplasm. Scale bars: 10 μm.
(b) Basal expression of *VQ9*.
(c) Expression of *VQ9* responding to abiotic stresses: RNA samples were prepared from 3-week-old wild-type seedlings at the given times after treatment with salt (250 mM NaCl), dehydration, cold (4°C) or heat (42°C).
(d) Expression of *VQ9* responding to pathogens. *Pseudomonas syringae* and *Botrytis cinerea* infections were performed as described previously (Chen *et al.*, 2010a). Error bars show standard deviations from three independent RNA extractions.

© 2013 The Authors

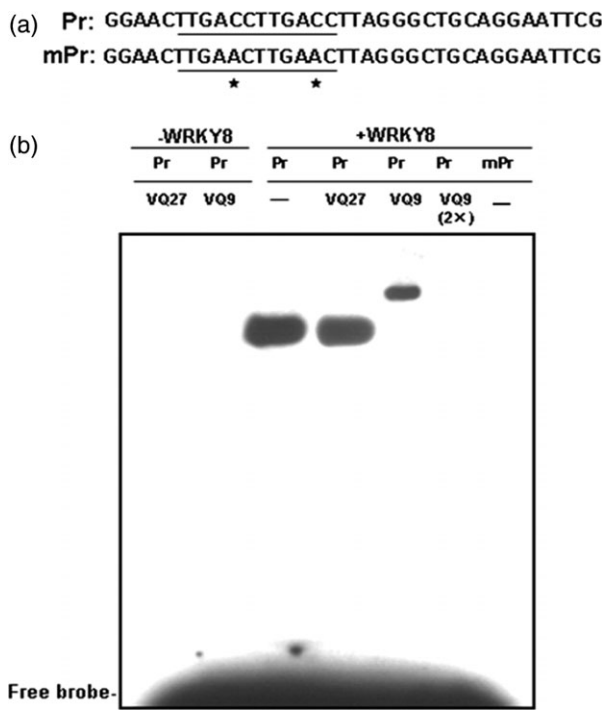

Figure 6. The DNA-binding activity of WRKY8 is decreased by VQ9.
(a) Oligonucleotides used in EMSA assay. The Pr probe contains two direct W-box repeats. In the mPr probe, TTGACC sequences are mutated to TTGAAC. Wild-type and mutated W-box sequences are underlined. *Mutated sites.
(b) EMSA of effects of VQ9 on binding activity of WRKY8. Recombinant 6 × His-tagged WRKY8 and VQ9 were purified and used for DNA binding assays. 6 × His-tagged VQ27 was included as a negative control. Binding assays were repeated twice with independently prepared recombinant proteins with similar results.

WRKY8. To test this possibility, we generated recombinant proteins in *Escherichia coli* and tested the WRKY8 binding activity to an oligonucleotide harboring two direct TTGACC W-box repeats (Pr; Figure 6a) using electrophoretic mobility shift assay (EMSA). Protein–DNA complexes with reduced migration were detected when WRKY8 was incubated with the DNA probe (Figure 6b); however, when the W-box sequences in the probes were changed from TTGACC to TTGAAC (mPr; Figure 6a), no binding complexes were detected (Figure 6b). These results suggested that the binding of WRKY8 to the W-box sequences is highly specific. When WRKY8 was combined with VQ9 in the binding reactions, we observed the formation of a super-shifted band with significantly lower intensity (Figure 6b). Moreover, when the protein level of VQ9 was doubled (2 × VQ9) in the assay, no visibly retarded band was observed (Figure 6b). Thus, the WRKY8–VQ9 interaction decreased the DNA-binding activity of WRKY8.

Disruption of VQ9 enhances tolerance to salinity stress

To study the role of VQ9 in salinity stress responses, we identified two T-DNA insertion mutants for *VQ9* and generated several *VQ9* overexpression lines (*VQ9*OE). The *vq9-1* mutant (CS853753) harbors a T-DNA insertion in the coding region (732 bp from the translation start), and *vq9-2* (CS857626) carries the T-DNA insertion in the promoter (−200 bp, relative to the translation start) (Figure 7a). qRT-PCRs were performed to compare the salt-induced accumulation of *VQ9* transcripts between the *vq9* mutant and the wild type. As shown in Figure 7(a), *VQ9* transcripts were detected at the expected induced levels in wild-type plants; however, few *VQ9* transcripts were detected in *vq9-1* in response to salt. In the *vq9-2* mutant, the NaCl-induced accumulation of *VQ9* transcripts was also reduced compared with the wild type (Figure 7a). The *VQ9*OE plants were confirmed by northern blot (Figure 8a). Two lines (*VQ9*OE-3 and -4) were selected for further analyses. Besides the changes in gene expression, there were no other obvious differences in morphology between the wild type and any mutant or transgenic line grown under normal growth conditions.

We next analyzed the performances of *vq9* mutants and *VQ9*OE lines under salinity stress. In the absence of salt, seed germination and early development were not affected in *vq9-1* or *vq9-2* mutants, compared with the wild type; however, on MS agar medium containing NaCl, both *vq9* mutants showed higher germination rates than those of the wild type (Figure 7b). Likewise, the post-germination growth of *vq9* mutants was also better than that of the wild type under salt stress (Figure 7c,d). Furthermore, the soil-grown *vq9* mutants were also more tolerant to salt stress than wild-type plants (Figure 7e–g). In contrast, the overexpression of *VQ9* rendered plants hypersensitive to salt stress (Figure 8). Thus, these results indicated that VQ9 functions as a negative regulator of salt stress in Arabidopsis.

Mutation of WRKY8 or VQ9 affects Na^+/K^+ homeostasis under salt stress

Maintaining ion homeostasis, especially a lower cytosolic Na^+/K^+ ratio, is a critical determinant of salt adaptation in plants. To determine whether WRKY8 and VQ9 participated in regulating ion homeostasis under salt stress, we determined the Na^+ and K^+ contents in *wrky8* and *vq9* mutants. When 3-week-old soil-grown plants were watered with H_2O, there were no significant differences in the Na^+ and K^+ contents between either of the mutants and the wild type (Figure 9a). Upon treatment with 150 mM NaCl, *wrky8* mutants accumulated less K^+ and substantially more Na^+, leading to an increased Na^+/K^+ ratio, whereas *vq9* mutants accumulated relatively more K^+ and less Na^+ (leading to a lower Na^+/K^+ ratio), compared with the wild type (Figure 9a,b). These observations suggested the possible involvement of WRKY8 and VQ9 in regulating Na^+/K^+ homeostasis under salt stress.

Recently, it was reported that K^+ deficiency in salt-sensitive plants partially results from greater K^+ loss

© 2013 The Authors

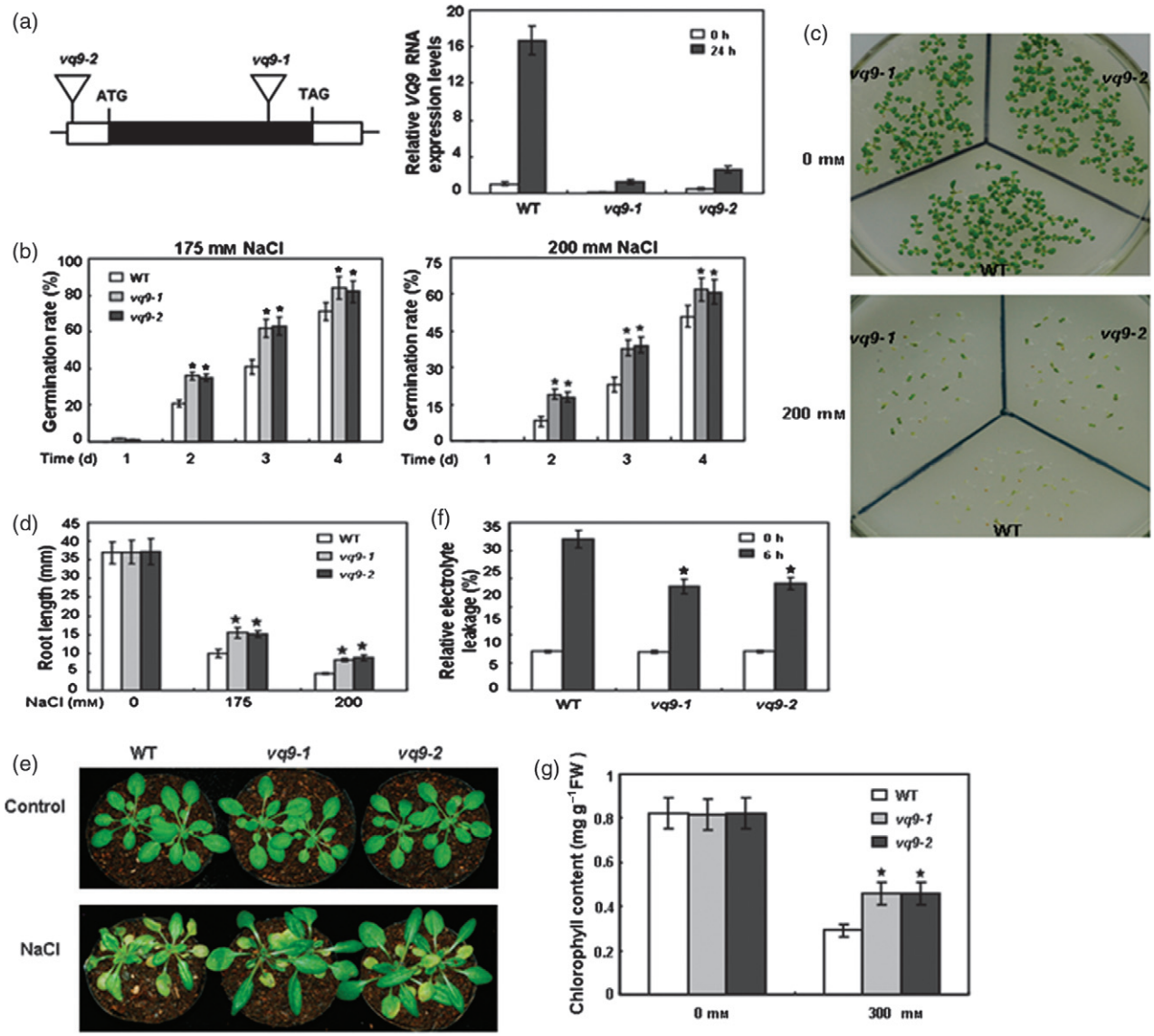

Figure 7. Enhanced tolerance of *vq9* mutants to salt stress.
(a) Isolation of *vq9* mutants. Diagram of *VQ9* and its T-DNA insertion mutants (left). qRT-PCR comparison of *VQ9* expression levels in the wild type (WT) and in *vq9* mutants (right). Error bars show standard deviations of three independent biological samples.
(b) Seed germination analyses. All experiments were performed three times, each evaluating more than 60 seeds; values are means ± SEs.
(c) Early seedling development analyses. WT and *vq9* mutant seeds were geminated in MS medium, and 3 days after stratification all were transferred to NaCl-containing medium. Pictures were taken 4 days after transfer.
(d) Root elongation analyses. Values shown are means ± SEs from three independent experiments.
(e) Salt-sensitivity analyses of soil-grown *vq9* mutants. After 3 weeks of growth in soil, the plants were watered with 300 mM NaCl for 18 days and photographed. Control plants were photographed before salt treatments. Experiments were repeated twice using over 50 plants per treatment.
(f) Relative electrolyte leakage analyses: 3-week-old plants were treated with 250 mM NaCl for 6 h; values shown are means ± SEs from three independent experiments.
(g) Chlorophyll content analyses: 3-week-old soil-grown plants were watered with 300 mM NaCl for 2 weeks and their chlorophyll contents were measured. Experiments were repeated three times. Values are means ± SEs. *Significant difference between mutant and WT ($P < 0.05$).

under salt stress (Chen *et al.*, 2005; Cuin *et al.*, 2008; Sun *et al.*, 2009). To further understand the function of WRKY8 and VQ9 in regulating Na^+/K^+ homeostasis, we investigated the salt shock-induced K^+ efflux in *wrky8-1* and *vq9-1* mutants. As shown in Figure 9(c), the net immediate K^+ efflux was higher in *wrky8-1* and lower in *vq9-1* compared with that in wild-type seedlings under NaCl treatment. This observation supported the involvement of WRKY8 and VQ9 in regulating Na^+/K^+ homeostasis under salt stress.

© 2013 The Authors

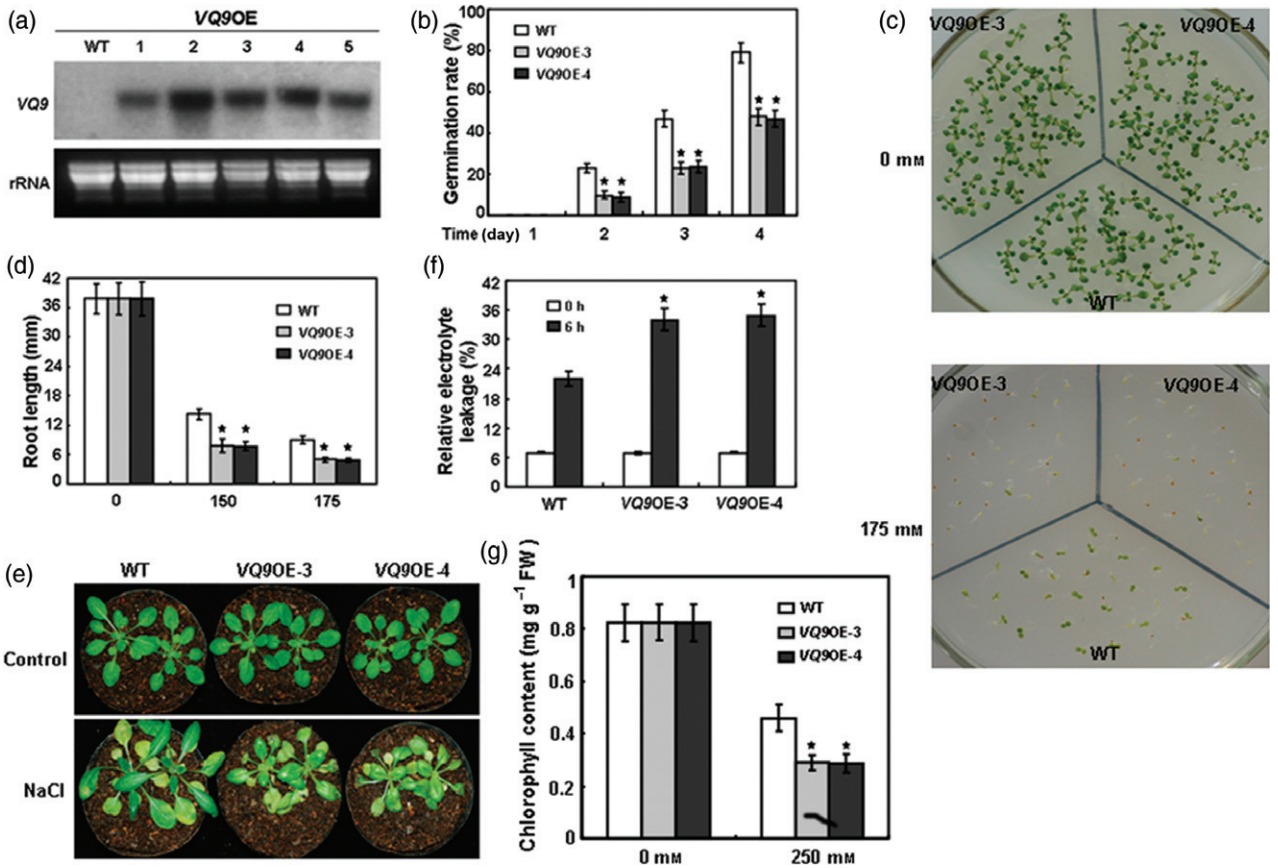

Figure 8. Phenotypic analyses of the *VQ9* overexpression plants.
(a) Northern blot analyses of *VQ9* expression in *VQ9* overexpression plants. RNA samples were prepared from leaves of five lines of *VQ9* overexpression plants or wild type (WT). A 20-μg portion of RNA was separated on an agarose-formaldehyde gel.
(b) Seed germination analyses: germination of WT and *VQ9*-overexpression lines on 175 mM NaCl medium over 4 days. All experiments were performed three times each, evaluating more than 60 seeds; values are means ± SEs.
(c) Early seedling development analyses: WT and *VQ9* overexpression plants were geminated in MS medium, and 3 days after stratification all were transferred to NaCl-containing medium. Pictures were taken 4 days after transfer.
(d) Root elongation analyses; values shown are means ± SEs from three independent experiments.
(e) Salt sensitivity analyses of soil-grown *VQ9* overexpression plants. After 3 weeks of growth in soil, the plants were watered with 250 mM NaCl for 18 days and photographed. Control plants were photographed before salt treatments. Experiments were repeated twice using over 50 plants per treatment.
(f) Relative electrolyte leakage analyses: 3-week-old plants were treated with 250 mM NaCl for 6 h; values shown are means ± SEs from three independent experiments.
(g) Chlorophyll contents analyses: the 3-week-old soil-grown plants were watered with 250 mM NaCl for 2 weeks and their chlorophyll contents were measured. Experiments were repeated three times. Values are means ± SEs. *VQ9*OE, *VQ9* overexpression plants. *Significant difference between mutant and WT ($P < 0.05$).

To further investigate the role of WRKY8 and VQ9 in Na^+/K^+ homeostasis, we analyzed the expression of *SOS1*, *SOS2* and *SOS3* in salt-stressed *wrky8* and *vq9* mutant seedlings. As shown in Figure 9(d), the expression levels were reduced in *wrky8* mutants but were increased in *vq9* mutants, compared with those in wild-type plants, under salt treatment. These results indicated that WRKY8 and VQ9 are involved in modulating the transcription of these genes.

WRKY8 directly binds the promoter of RD29A *in vivo*

The salt-stress response phenotypes of the *wrky8* and *vq9* mutants suggested that the expression of stress-responsive genes might be altered in the mutants. To test this possibility, we examined the expression of several stress-inducible genes in *wrky8* and *vq9* mutants with or without NaCl treatment. *RD29A*, *RD29B*, *RD20* and *ADH1* are well-characterized marker genes with protective functions against stress damage. As shown in Figure 10(a), the basic expression levels of these stress-responsive genes were generally low, and were not affected in *wrky8* and *vq9* mutants; however, under salinity stress, their transcripts were reduced in *wrky8* mutants and enhanced in *vq9* mutants, compared with wild-type plants (Figure 10a). These results suggested that WRKY8 and VQ9 function antagonistically to regulate the expression of downstream stress-responsive genes, which may

© 2013 The Authors

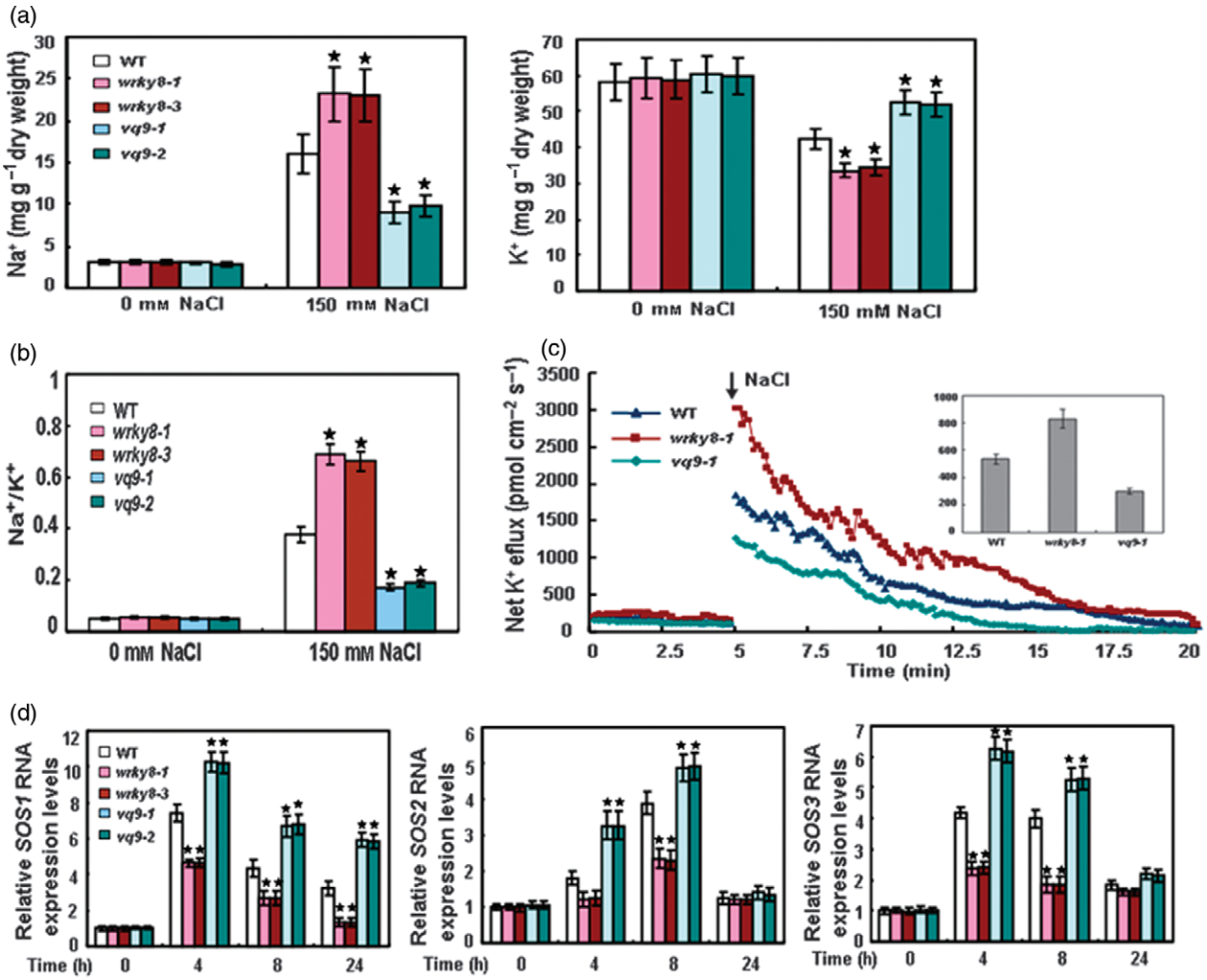

Figure 9. Na^+/K^+ homeostasis in *wrky8* and *vq9* mutants, and in the wild type (WT).
(a) Na^+ and K^+ contents: 3-week-old soil-grown plants were watered with 0 mM or 150 mM NaCl solution and samples were harvested 5 days later. Values shown are means ± SEs from three independent experiments.
(b) Na^+/K^+ ratio.
(c) Net K^+ efflux in root tips. Seeds were germinated on MS agar medium for 4 days in a vertical manner. The net immediate K^+ efflux was measured using the non-injuring technique after the addition of salt. The insert shows the mean efflux rates within the measuring period of 0–20 min.
(d) Expression of *SOS1*, *SOS2* and *SOS3*. Error bars show standard deviations from three independent RNA extractions. *Significant difference between mutant and WT ($P < 0.05$).

partially account for the contrasting responses of *wrky8* and *vq9* to salt stress.

The WRKY factors can directly bind the W-box elements of downstream target-gene promoters. Examination of the promoters of *RD29A*, *RD29B*, *RD20* and *ADH1* genes revealed the presence of W-boxes (Figure 10b). We conducted chromatin immunoprecipitation (ChIP) assays to investigate whether these genes were directly regulated by WRKY8. For this experiment, we created a transgenic line expressing a WRKY8 cDNA construct with an N-terminal hemagglutinin (HA) tag under the control of its native promoter (designated as HA-WRKY8). The presence of the HA tag allowed us to immunoprecipitate the WRKY8–DNA complex using a commercial anti-HA antibody. As shown in Figure 10(c), the ChIP-quantitative PCR (ChIP-qPCR) analyses showed that WRKY8 interacted with one W-box element in the promoter of *RD29A* after NaCl treatment. These results suggested that WRKY8 directly regulates *RD29A* transcription under salt stress.

DISCUSSION

Previously, we showed that Arabidopsis *WRKY8* participated in regulating defense responses (Chen *et al.*, 2010a). In this study, we further investigated its expression patterns. Higher levels of *WRKY8* transcripts accumulated in roots and in salt-treated plants (Figure 1); however, the expression of *WRKY8* was not upregulated by osmotic stress, dehydration, cold or heat (Figure 1b). These results

© 2013 The Authors

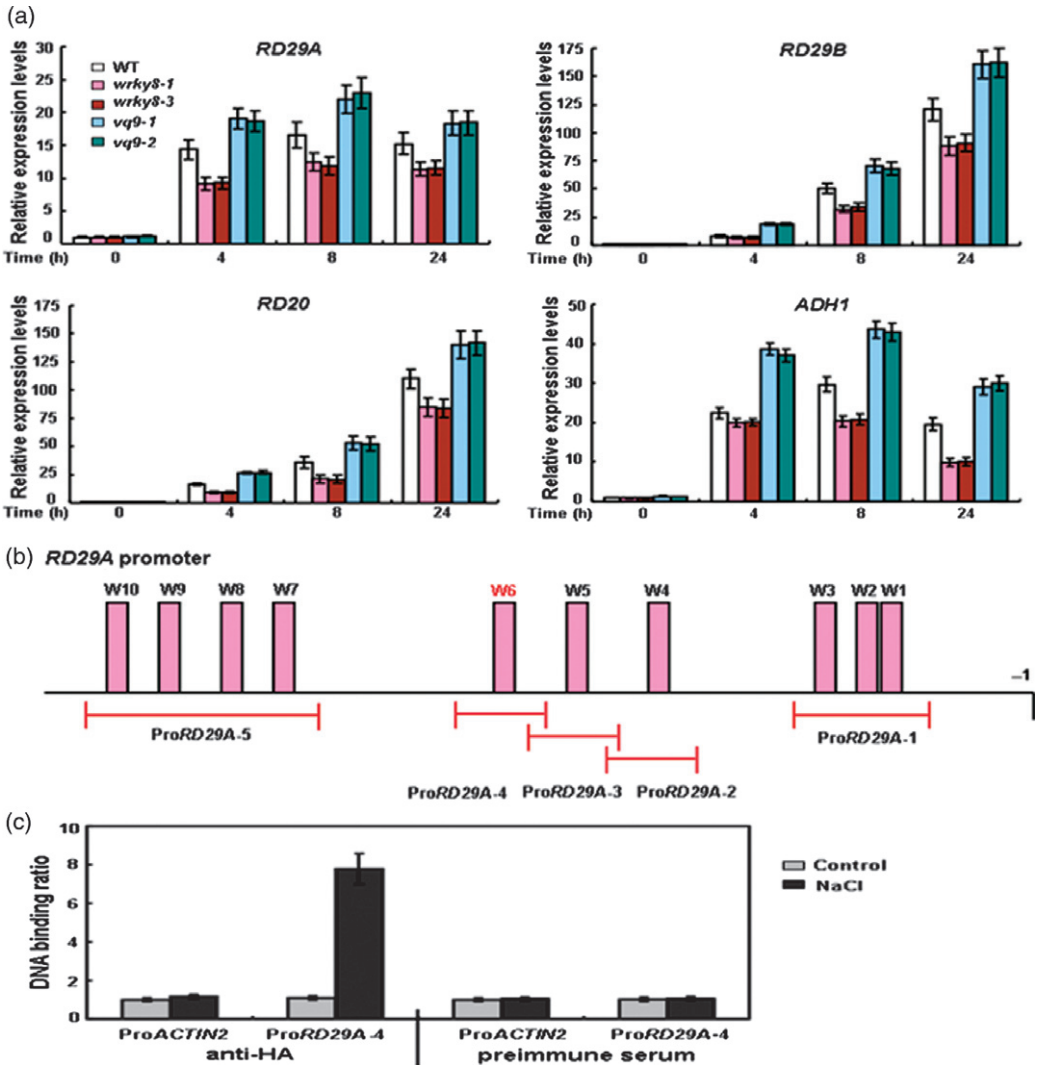

Figure 10. Direct binding of WRKY8 to the promoter of *RD29A*.
(a) Expression of stress-responsive genes. The relative expression levels of *RD29A*, *RD29B*, *RD20* and *ADH1* in salt-stressed plants were analyzed by qRT-PCR. Error bars show standard deviations from three independent RNA extractions. WT, wild type. *Significant difference between mutant and wild type ($P < 0.05$).
(b) Promoter structure of *RD29A*. W1, W2…, denote each W-box, numbered from right to left, with sequence sites relative to the start codon. The W6 in red is the binding site of WRKY8. Red lines indicate sequences detected by ChIP assays, as described in Table S3. In promoter fragment names, the prefix 'Pro' indicates a promoter.
(c) WRKY8 interacts with the promoter of *RD29A*. ChIP-qPCR analyses of the DNA binding ratio of WRKY8 to the promoter of *RD29A*. To confirm the specificity of anti-HA antibody, pre-immune serum was used as a negative control. *ACTIN2* promoter (Pro*ACTIN2*) was used as a control for ChIP-qPCR.

suggested that the *WRKY8* gene mainly responds to high salinity during certain abiotic stress treatments. Phenotype analyses showed that the *wrky8* mutants germinated later than the wild type in the presence of salt, particularly on high-salt medium (Figure 2a). Both mutants were also hypersensitive to salt stress during post-germination development and vegetative growth stages (Figure 2b–g). Thus, the NaCl-responsive WRKY8 factor functions as a positive modulator of salt stress tolerance.

There is increasing evidence that WRKY proteins regulate multiple abiotic stress responses (Chen *et al.*, 2012). Intriguingly, the majority of these functionally characterized WRKY factors act as positive regulators to stimulate the tolerance of plants to environmental stresses (Devaiah *et al.*, 2007; Chen *et al.*, 2010b; Li *et al.*, 2010; Ren *et al.*, 2010). For example, WRKY75 positively regulated Pi-starvation responses (Devaiah *et al.*, 2007). Moreover, the overexpression of several *WRKY* genes in Arabidopsis significantly increased tolerance to drought, salt or osmotic stress (Qiu and Yu, 2009; Song *et al.*, 2009; Niu *et al.*, 2012). Nevertheless, several factors in this family are thought to negatively mediate abiotic stress responses (Wei *et al.*, 2008; Zou *et al.*, 2010), and some members have dual regulatory activities, acting as both positive and

© 2013 The Authors

negative modulators in response to different abiotic stresses (Kasajima and Fujiwara, 2007; Chen *et al.*, 2009; Kasajima *et al.*, 2010). The multiple roles of WRKY proteins suggest that the complex signaling and transcriptional networks of abiotic stress responses require tight regulation. We speculate that WRKY proteins may play crucial roles in maintaining the appropriate balance among different stress-signaling pathways to establish tolerance, while minimizing detrimental effects on plant growth and development. However, the exact mechanisms underlying the involvement of WRKY factors in stress responses remain unclear. Further research is required to identify putative proteins interacting with WRKY factors and to identify their downstream targets.

Using a yeast two-hybrid assay, we identified VQ9 as an interacting partner of WRKY8 (Figure 4a). Further investigation showed that WRKY8 and VQ9 formed a complex in the nucleus (Figure 4b,c). As VQ9 lacked the predicted nuclear localization signals, we analyzed its subcellular localization. The VQ9-GFP fusion protein was exclusively localized in the nucleus (Figure 5a), consistent with its ability to interact with WRKY8 *in vivo*. The *VQ9* gene was also highly expressed in roots and strongly responded to salinity stress (Figure 5b,c), sharing similar spatial and temporal expression patterns with *WRKY8*; however, unlike salt-sensitive *wrky8* mutants, *vq9* mutants were more tolerant to salinity stress than the wild type (Figure 7). Thus, the nuclear-localized salt-responsive VQ9 acts antagonistically with WRKY8 to mediate salt stress responses.

VQ9 is one member of a family of plant proteins that share a conserved VQ motif (FXXXVQXXTG). This family has more than 30 representatives in Arabidopsis (Xie *et al.*, 2010; Cheng *et al.*, 2012). Besides VQ9, several members of this family have been shown to interact with WRKY factors to mediate defense responses or development (Andreasson *et al.*, 2005; Wang *et al.*, 2010; Lai *et al.*, 2011). Cheng *et al.* (2012) recently showed that VQ proteins may interact with several members of group I and group IIc WRKY factors in yeast; however, the interactions between WRKY factors and VQ proteins in a given type of cell or tissue under given conditions remain largely unclear. In this study, we identified a new partnership between WRKY8 and VQ9 to mediate salt stress responses. Our results showed that the interaction of WRKY8 with VQ9 was specific, as WRKY8 didn't interact with the other VQ family member tested (Figure 4). Moreover, the majority of VQ proteins may not form a protein complex with WRKY8 under high-salt conditions, as microarray expression analyses revealed that most *VQ* genes were not induced by salt treatments (Kreps *et al.*, 2002; Jiang and Deyholos, 2006; Ma *et al.*, 2006). For example, VQ32, a structural homolog of VQ9, was not responsive to NaCl treatment (Figure S3), indicating that it may not interact with WRKY8 under high-salt conditions. Hence, further research is required to investigate the exact interactions between WRKY and VQ proteins in a physiological context, and to illustrate the biological functions of VQ proteins.

The EMSA assays showed that VQ9 decreased the DNA-binding activity of WRKY8 (Figure 6), suggesting that their interaction may lead to the inactivation of WRKY8. Likewise, the WRKY53-interacting ESR inhibited DNA-binding of WRKY53 and functioned as a negative regulator of WRKY53 in leaf senescence (Miao and Zentgraf, 2007). Overexpression of HDA19 effectively abolished the transcriptional activation activity of its interacting partners WRKY38 and WRKY62 during defense responses (Kim *et al.*, 2008). Therefore, physical interactions between WRKY factors and other proteins may provide specific mechanisms to inhibit their DNA-binding and/or transcriptional activities, finely balancing the different stress-signaling pathways. The characterization of these physical interactions may shed new light on the molecular basis of the tight regulation of stress-signal transduction.

To minimize the adverse effects of salt stress, plants have evolved various adaptive mechanisms. The maintenance of ion homeostasis, especially the maintenance of a low Na^+/K^+ concentration ratio, is a pivotal strategy for plants to grow in high-salt conditions. A high Na^+/K^+ concentration ratio is toxic to plants, inhibiting various processes such as K^+ absorption (Rains and Epstein, 1965), vital enzyme reactions (Murguía *et al.*, 1995), protein synthesis (Hall and Flowers, 1973) and photosynthesis (Tsugane *et al.*, 1999). As shown in Figure 9(a) and (b), compared with that of the wild type, the Na^+/K^+ concentration ratio was higher in *wrky8* mutants but lower in *vq9* mutants under high-salt conditions. Further investigation revealed that the net K^+ efflux was higher in *wrky8-1* but lower in *vq9-1* than that in the wild type under NaCl treatment (Figure 9c). These results suggested that WRKY8 and VQ9 regulate Na^+/K^+ homeostasis under salt stress. Previous studies have revealed that the SOS pathway plays critical roles in regulating ion homeostasis to confer salt tolerance (Qiu *et al.*, 2004; Mahajan *et al.*, 2008). Expression analyses showed that the expression levels of *SOS1*, *SOS2* and *SOS3* were reduced in *wrky8* mutants, but increased in *vq9* mutants, compared with those in wild-type seedlings under salt treatment (Figure 9d); however, further ChIP-qPCR analyses showed that WRKY8 didn't interact with their promoters, indicating that WRKY8 indirectly regulates their transcription under salt stress. Further study is needed to illustrate the regulatory relationship between WRKY8 and those *SOS* genes.

To gain insight into the molecular basis of the functions of WRKY8 and VQ9 in salinity stress responses, we analyzed the expression of several well-characterized marker genes in *wrky8* and *vq9* mutants. The expression of *RD29A*, *RD29B*, *RD20* and *ADH1* was reduced in *wrky8* mutants but was increased in *vq9* mutants, compared with

© 2013 The Authors

that in wild-type plants, under salt treatment (Figure 10a). Moreover, our results showed that the promoter of *RD29A* could be directly recognized by WRKY8 (Figure 10b,c). These data suggest that the WRKY8 factor and VQ9 protein may modulate salt stress responses partially through altering expressions of downstream stress-related genes, especially the direct target *RD29A*. Abscisic acid (ABA) is an important hormone that regulates many essential processes, including the inhibition of germination, maintenance of seed dormancy, regulation of stomatal behavior and adaptive responses to environmental stresses (Finkelstein *et al.*, 2002). To understand whether WRKY8 and VQ9 was involved in ABA signaling, we analyzed the expression of several ABA-responsive transcription factors, including *ABF1*, *ABF2*, *ABF3*, *ABF4*, *ABI5* and *AREB3*, in salt-stressed *wrky8* and *vq9* mutants. As shown in Figure S4, their expression levels did not differ between any of the mutant and the wild type. This result suggested that WRKY8 and VQ9 might function independently on ABA signaling to mediate salinity stress responses.

EXPERIMENTAL PROCEDURES

Materials and plant growth conditions

Common chemicals were obtained from the Shanghai Sangon Biotechnology Co. Ltd. (http://www.sangon.com) Arabidopsis plants were grown in an artificial growth chamber at 22°C with a photoperiod of 10 h of light and 14 h of darkness. The wild-type plants and all mutants used in this study were in the Columbia (Col-0) genetic background.

Abiotic stress treatments

We used 3-week-old Arabidopsis grown on soil for expression analyses under various abiotic stress treatments. Plants were exposed to high salinity (250 mM NaCl), 25% polyethylene glycol (PEG) , cold (4°C) or heat (42°C). Whole seedlings were harvested at given times after treatments.

Northern blot

The RNA (20 μg) was separated on an agarose-formaldehyde gel and then transferred onto nylon membranes, which were hybridized and washed as described by Hu *et al.* (2012). Transcripts for *VQ9* and *VQ32* were detected using their full-length cDNA as probes, which were labeled by [α-^{32}P]dATP using the TaKaRa Random Primers DNA Labeling System (TaKaRa Bio Inc., http://www.takara-bio.com).

qRT-PCR

qRT-PCR was performed as described by Hu *et al.* (2012). Briefly, first-strand cDNA was synthesized from 1.5 μg DNase-treated RNA in a 20-μl reaction volume using M-MuLV reverse transcriptase (Fermentas, now Thermo Scientific, http://www.thermoscientificbio.com) with oligo(dT)18 primer. qRT-PCR was performed with double-strength SYBR Green I master mix on a Roche LightCycler 480 real-time PCR machine (Roche, http://www.roche.com). *ACTIN2* was used as a control. Gene-specific primers used to detect transcripts are listed in Table S1.

Identification of T-DNA insertion mutants and construction of overexpression plants

The *vq9-1* and *vq9-2* lines were from the Arabidopsis Resource Center at Ohio State University (http://abrc.osu.edu). We confirmed the T-DNA insertions by PCR using a combination of a gene-specific primer and a T-DNA border primer (5′-AAAC GTCCGCAATGTGTTAT-3′). The homozygosity of the mutants was identified by PCR using a pair of primers corresponding to sequences flanking the T-DNA insertion sites. To generate the *VQ9* overexpression transgenic plants, the full-length cDNA of *VQ9* was cloned into the pOCA30 vector in the sense orientation behind the CaMV *35S* promoter (Chen and Chen, 2002). The recombinant plasmids were introduced into *Agrobacterium tumefaciens* GV3101 and used to transform Arabidopsis.

Relative electrolyte leakage and chlorophyll content measurement

To measure relative electrolyte leakage, 3-week-old plants were treated with 250 mM NaCl. After 6 h, rosette leaves were harvested to measure relative electrolyte leakage according to the method described by Jiang *et al.* (2007). Chlorophyll was extracted with 80% acetone from leaves of salt-treated plants. Chlorophyll content was determined at 663 and 645 nm according to the method described by Lichtenthaler (1987).

Yeast two-hybrid screening and confirmation

The truncated *WRKY8* cDNA was cloned into the bait pGBKT7 vector, and then transformed into the yeast strain Y2HGold. The cDNA library was prepared from 3-week-old salt-stressed Arabidopsis and cloned into the pGADT7-Rec vector. Two-hybrid screening was performed as described in Clontech's Matchmaker™ Gold Yeast Two-Hybrid user manual (Clontech, http://www.clontech.com). To confirm the interactions, the full-length *VQ9* or *VQ27* CDS sequences were cloned into the prey pGADT7 vector. The primers used for amplifying these truncated or mutated fragments were listed in Table S2.

BiFC

cDNA sequences of the N-terminal, 173-amino acid, enhanced YFP (N-YFP), and C-terminal, 64-amino acid (C-YFP) fragments were cloned into pFGC5941 to generate pFGC-N-YFP and pFGC-C-YFP, respectively (Kim *et al.*, 2008). The full-length *WRKY8* CDS sequence was inserted into pFGC-C-YFP to generate the C-terminal in-frame fusions with C-YFP, whereas *VQ9* and *VQ27* CDS sequences were introduced into pFGC-N-YFP to form N-terminal in-frame fusions with N-YFP. The plasmids were introduced into *A. tumefaciens* GV3101, and infiltration of *N. benthamiana* was performed as described previously (Kim *et al.*, 2008). Infected tissues were analyzed at 48 h after infiltration. Fluorescence and DAPI were observed under a confocal laser scanning microscope (Olympus, http://www.olympus-global.com).

CoIP

The full-length CDS of *WRKY8*, *VQ9* or *VQ27* were cloned into a tagging plasmid behind the MYC or FLAG tag sequence in the sense orientation behind the CaMV *35S* promoter. The constructs were transformed into *A. tumefaciens* GV3101. MYC-fused WRKY8 and FLAG-fused VQ9 or VQ27 were then transiently co-expressed in *N. benthamiana*. For transient expression, leaves were infiltrated with the bacterial cell suspensions as described previously

© 2013 The Authors

(Kim *et al.*, 2008). CoIP assays were performed using leaf protein extracts as described in a previous study (Shang *et al.*, 2010). Briefly, MYC-fused WRKY8 was immunoprecipitated using the anti-MYC antibody and the co-immunoprecipitated protein was then detected using an anti-FLAG rabbit antibody (Sigma–Aldrich, http://www.sigmaaldrich.com).

Subcellular localization

The full-length or mutated CDS of *VQ9* were cloned into a GFP vector and subcloned into pOCA30 (Chen and Chen, 2002). The constructs were then transformed into *A. tumefaciens* GV3101. For transient expression in *N. benthamiana*, leaves were infiltrated with the bacterial cell suspensions [OD_{600} = 0.05, 10 mM 2-(*N*-morpholino)ethanesulfonic acid (MES), 10 mM $MgCl_2$ and 100 μM acetosyringone]. Infected leaves were sectioned 48 h after infiltration. Fluorescence and DAPI were observed under a confocal laser scanning microscope (Olympus).

EMSA

The full-length CDS of *WRKY8, VQ9* and *VQ27* were subcloned into the expression vector pET-32a (Novagen, now EMD Millipore, http://www.emdmillipore.com) and transformed into *E. coli* strain BL21 (DE3). Expression of the recombinant proteins was induced by isopropyl β-D-1-thiogalactopyranoside (IPTG). The expressed proteins were purified according to the manual provided by Novagen. The EMSA assay was carried out using the Light Shift Chemiluminescent EMSA Kit (20 148; Pierce, http://www.piercenet.com) according to the manufacturer's instructions.

The determination of Na^+ and K^+ contents and net K^+ efflux measurements

Three-week-old soil-grown plants were watered with 0 mM or 150 mM NaCl solution, and samples were harvested 5 days later. The Na^+ and K^+ contents were determined by inductively coupled plasma atomic emission spectrometry (ThermoFisher Scientific, http://www.thermofisher.com). The net flux of K^+ was measured non-invasively by Xuyue-Sci. & Tech. Co. (Beijing, China, http://www.xuyue.net), with non-invasive micro-test technology (NMT, Younger USA Sci. and Tech. Corp., Amherst, MA, USA, http://www.youngerusa.com) as described previously (Sun *et al.*, 2009; Xu *et al.*, 2011). Seeds of mutants and wild type were germinated on MS agar medium for 4 days in a vertical manner. The net immediate K^+ efflux was measured using the non-injuring technique after the addition of salt (with a final NaCl concentration in the buffer of 175 mM). The concentration gradients of the target ion were measured by moving the ion-selective microelectrode between two positions close to the plant material in a preset path, with a distance of 20 μm; the whole cycle was completed in 5.25 sec.

ChIP analyses

For ChIP analyses, a transgenic line was created expressing WRKY8 with an N-terminal HA tag under its native promoter. ChIP assays were performed as described in previous studies (Saleh *et al.*, 2008; Shang *et al.*, 2010). To quantify the WRKY8-DNA binding ratio, ChIP-qPCR analyses were performed as described previously with the *ACTIN2* 3′-untranslated region as the endogenous control (Mukhopadhyay *et al.*, 2008). The primers used for the amplification of the promoter fragment of *ACTIN2* were as follows: 5′-CGTTTCGCTTTCCT-3′ and 5′-AACGACTAACGAGCAG-3′. The results presented were obtained from at least three independent experiments.

Accession numbers

Arabidopsis Genome Initiative numbers for the genes discussed in this article are as follows: *WRKY8* (AT5G46350), *VQ9* (At1g78310), *VQ27* (At4g15120), *VQ32* (At5g46780), *SOS1* (AT2G01980), *SOS2* (AT5G35410), *SOS3* (AT5G24270), *RD29A* (AT5G52310), *RD29B* (AT5G52300), *RD20* (AT2G33380), *ADH1* (AT1G77120), *ABF1* (AT1G49720), *ABF2* (AT1G45249), *ABF3* (AT4G34000), *ABF4* (AT3G19290), *ABI5* (AT2G36270), *AREB3* (AT3G56850) and *ACTIN2* (AT3G18780).

ACKNOWLEDGEMENTS

We thank the Arabidopsis Resource Center at Ohio State University for the *wrky8* and *vq9* mutants. The authors also thank Dr Zhixiang Chen (Purdue University, USA) for BiFC vectors, and staff of the Biogeochemical Laboratory (Xishuangbanna Tropical Botanical Garden, China) for their assistance in the determination of iron contents. There is no conflict of interest. This work was supported by the Natural Science Foundation of China (30771223) and the Science Foundation of the Chinese Academy of Sciences (KSCX3-EW-N-07 and the CAS 135 program XTBG-F04).

SUPPORTING INFORMATION

Additional Supporting Information may be found in the online version of this article.

Figure S1. Statistical analyses of transformed tobacco cells with fluorescence.

Figure S2. Yeast two-hybrid assays to identify the regions of WRKY8 and VQ9 required for interaction.

Figure S3. Expression profiles of *VQ32*.

Figure S4. Expression analyses of ABA-responsive transcription factors.

Table S1. Primers used for qRT-PCR.

Table S2. Primers used for generating truncated WRKY8 or VQ9 constructs for yeast two-hybrid assays.

Table S3. Information for detecting the WRKY8-binding promoter sequences.

REFERENCES

Andreasson, E., Jenkins, T., Brodersen, P. *et al.* (2005) The MAP kinase substrate MKS1 is a regulator of plant defense responses. *EMBO J.* **24**, 2579–2589.

Birkenbihl, R.P., Diezel, C. and Somssich, I.E. (2012) Arabidopsis WRKY33 is a key transcriptional regulator of hormonal and metabolic responses toward *Botrytis cinerea* infection. *Plant Physiol.* **159**, 266–285.

Bray, E.A., Bailey-Serres, J. and Weretilnyk, E. (2000) Responses to abiotic stresses. In *Biochemistry and Molecular Biology of Plants* (Buchanan, B.B., Gruissem, W. and Jones, R.L., eds). Rockville, MD: American Society of Plant Physiologists, pp. 1158–1249.

Chen, C. and Chen, Z. (2002) Potentiation of developmentally regulated plant defense response by AtWRKY18, a pathogen-induced Arabidopsis transcription factor. *Plant Physiol.* **129**, 706–716.

Chen, Z., Newman, I., Zhou, M., Mendham, N., Zhang, G. and Shabala, S. (2005) Screening plants for salt tolerance by measuring K^+ flux: a case study for barley. *Plant Cell Environ.* **28**, 1230–1246.

Chen, Y., Li, L., Xu, Q., Kong, Y., Wang, H. and Wu, W. (2009) The WRKY6 transcription factor modulates *PHOSPHATE1* expression in response to low Pi stress in Arabidopsis. *Plant Cell*, **21**, 3554–3566.

Chen, L., Zhang, L. and Yu, D. (2010a) Wounding-induced WRKY8 is involved in basal defense in Arabidopsis. *Mol. Plant Microbe Interact.* **23**, 558–565.

Chen, H., Lai, Z., Shi, J., Xiao, Y., Chen, Z. and Xu, X. (2010b) Roles of Arabidopsis WRKY18, WRKY40 and WRKY60 transcription factors in plant responses to abscisic acid and abiotic stress. *BMC Plant Biol.* **10**, 281.

© 2013 The Authors

Chen, L., Song, Y., Li, S., Zhang, L., Zou, C. and Yu, D. (2012) The role of WRKY transcription factors in plant abiotic stresses. *Biochim. Biophys. Acta* **1819**, 120–128.

Cheng, Y., Zhou, Y., Yang, Y. *et al.* (2012) Structural and functional analysis of VQ motif-containing proteins in Arabidopsis as interacting proteins of WRKY transcription factors. *Plant Physiol.* **159**, 810–825.

Cheong, M.S. and Yun, D.J. (2007) Salt-stress signaling. *J. Plant Biol.* **50**, 148–155.

Cuin, T.A., Betts, S.A., Chalmandrier, R. and Shabala, S. (2008) A root's ability to retain K^+ correlates with salt tolerance in wheat. *J. Exp. Bot.* **59**, 2697–2706.

Devaiah, B.N., Karthikeyan, A.S. and Raghothama, K.G. (2007) WRKY75 transcription factor is a modulator of phosphate acquisition and root development in Arabidopsis. *Plant Physiol.* **143**, 1789–1801.

Eulgem, T., Rushton, P.J., Robatzek, S. and Somssich, I.E. (2000) The WRKY superfamily of plant transcription factors. *Trends Plant Sci.* **5**, 199–206.

Finkelstein, R.R., Gamplal, S.S. and Rock, C.D. (2002) Abscisic acid signaling in seeds and seedlings. *Plant Cell*, **14**(Suppl.), S15–S45.

Hall, J.L. and Flowers, T.J. (1973) The effect of salt on protein synthesis in the halophyte *Suaeda maritima*. *Planta*, **110**, 361–368.

Hu, Y., Dong, Q. and Yu, D. (2012) Arabidopsis WRKY46 coordinates with WRKY70 and WRKY53 in basal resistance against pathogen *Pseudomonas syringae*. *Plant Sci.* **185–186**, 288–297.

Jiang, Y. and Deyholos, M.K. (2006) Comprehensive transcriptional profiling of NaCl-stressed Arabidopsis roots reveals novel classes of responsive genes. *BMC Plant Biol.* **6**, 25.

Jiang, Y., Yang, B., Harris, N.S. and Deyholos, M.K. (2007) Comparative proteomic analysis of NaCl stress-responsive proteins in Arabidopsis roots. *J. Exp. Bot.* **58**, 3591–3607.

Journot-Catalino, N., Somssich, I.E., Roby, D. and Kroj, T. (2006) The transcription factors WRKY11 and WRKY17 act as negative regulators of basal resistance in *Arabidopsis thaliana*. *Plant Cell*, **18**, 3289–3302.

Kasajima, I. and Fujiwara, T. (2007) Microarray analysis of B nutrient response: identification of several high-B inducible genes and roles of WRKY6 in low-B response. *Plant Cell Physiol.* **48**, S46–S46.

Kasajima, I., Ide, Y., Yokota Hirai, M. and Fujiwara, T. (2010) WRKY6 is involved in the response to boron deficiency in *Arabidopsis thaliana*. *Physiol. Plant.* **139**, 80–92.

Kim, K.C., Lai, Z., Fan, B. and Chen, Z. (2008) Arabidopsis WRKY38 and WRKY62 transcription factors interact with histone deacetylase 19 in basal defense. *Plant Cell*, **20**, 2357–2371.

Kreps, J.A., Wu, Y., Chang, H.S., Zhu, T., Wang, X. and Harper, J.F. (2002) Transcriptome changes for Arabidopsis in response to salt, osmotic, and cold stress. *Plant Physiol.* **130**, 2129–2141.

Lai, Z., Li, Y., Wang, F., Cheng, Y., Fan, B., Yu, J.Q. and Chen, Z. (2011) Arabidopsis sigma factor binding proteins are activators of the WRKY33 transcription factor in plant defense. *Plant Cell*, **23**, 3824–3841.

Li, S., Zhou, X., Chen, L., Huang, W. and Yu, D. (2010) Functional characterization of *Arabidopsis thaliana* WRKY39 in heat stress. *Mol. Cells* **29**, 475–483.

Li, S., Fu, Q., Chen, L., Huang, W. and Yu, D. (2011) *Arabidopsis thaliana* WRKY25, WRKY26, and WRKY33 coordinate induction of plant thermotolerance. *Planta*, **233**, 1237–1252.

Li, G., Meng, X., Wang, R., Mao, G., Han, L., Liu, Y. and Zhang, S. (2012) Dual-level regulation of ACC synthase activity by MPK3/MPK6 cascade and its downstream WRKY transcription factor during ethylene induction in Arabidopsis. *PLoS Genet.* **8**, e1002767.

Lichtenthaler, H.K. (1987) Chlorophylls and carotenoids pigments of photosynthetic biomembranes. *Methods Enzymol.* **148**, 350–382.

Ma, S., Gong, Q. and Bohnert, H.J. (2006) Dissecting salt stress pathways. *J. Exp. Bot.* **57**, 1097–1107.

Mahajan, S., Pandey, G.K. and Tuteja, N. (2008) Calcium- and salt stress signaling in plants: shedding light on SOS pathway. *Arch. Biochem. Biophys.* **471**, 146–158.

Miao, Y. and Zentgraf, U. (2007) The antagonist function of Arabidopsis WRKY53 and ESR/ESP in leaf senescence is modulated by the jasmonic and salicylic acid equilibrium. *Plant Cell*, **19**, 819–830.

Mukhopadhyay, A., Deplancke, B., Walhout, A.J. and Tissenbaum, H.A. (2008) Chromatin immunoprecipitation (ChIP) coupled to detection by quantitative real-time PCR to study transcription factor binding to DNA in *Caenorhabditis elegans*. *Nat. Protoc.* **3**, 698–709.

Munns, R. and Tester, M. (2008) Mechanisms of salinity tolerance. *Annu. Rev. Plant Biol.* **59**, 651–681.

Murguía, J.R., Bellés, J.M. and Serrano, R. (1995) A salt-sensitive 3′(2′), 5′-bisphosphate nucleotidase involved in sulfate activation. *Science*, **267**, 232–234.

Niu, C., Wei, W., Zhou, Q. *et al.* (2012) Wheat WRKY genes *TaWRKY2* and *TaWRKY19* regulate abiotic stress tolerance in transgenic Arabidopsis plants. *Plant, Cell Environ.* **35**, 1156–1170.

Pandey, S.P. and Somssich, I.E. (2009) The role of WRKY transcription factors in plant immunity. *Plant Physiol.* **150**, 1648–1655.

Pandey, S.P., Roccaro, M., Schön, M., Logemann, E. and Somssich, I.E. (2010) Transcriptional reprogramming regulated by WRKY18 and WRKY40 facilitates powdery mildew infection of Arabidopsis. *Plant J.* **64**, 912–923.

Qiu, Y. and Yu, D. (2009) Over-expression of the stress-induced *OsWRKY45* enhances disease resistance and drought tolerance in Arabidopsis. *Environ. Exp. Bot.* **65**, 35–47.

Qiu, Q.S., Guo, Y., Quintero, F.J., Pardo, J.M., Schumaker, K.S. and Zhu, J.K. (2004) Regulation of vacuolar Na^+/H^+ exchange in *Arabidopsis thaliana* by the salt-overly-sensitive (SOS) pathway. *J. Biol. Chem.* **279**, 207–215.

Rains, D.W. and Epstein, E. (1965) Transport of sodium in plant tissue. *Science*, **148**, 1611.

Ren, X., Chen, Z., Liu, Y., Zhang, H., Zhang, M., Liu, Q., Hong, X., Zhu, J.K. and Gong, Z. (2010) ABO3, a WRKY transcription factor, mediates plant responses to abscisic acid and drought tolerance in Arabidopsis. *Plant J.* **63**, 417–429.

Rushton, P.J., Somssich, I.E., Ringler, P. and Shen, Q.J. (2010) WRKY transcription factors. *Trends Plant Sci.* **15**, 247–258.

Saleh, A., Alvarez-Venegas, R. and Avramova, Z. (2008) An efficient chromatin immunoprecipitation (ChIP) protocol for studying histone modifications in Arabidopsis plants. *Nat. Protoc.* **3**, 1018–1025.

Shang, Y., Yan, L., Liu, Z. *et al.* (2010) The Mg-chelatase H subunit of Arabidopsis antagonizes a group of WRKY transcription repressors to relieve ABA-responsive genes of inhibition. *Plant Cell*, **22**, 1909–1935.

Song, Y., Jing, S. and Yu, D. (2009) Overexpression of the stress induced *OsWRKY08* improves the osmotic stress tolerance in Arabidopsis. *Chin. Sci. Bull.* **54**, 4671–4678.

Sun, J., Dai, S., Wang, R. *et al.* (2009) Calcium mediates root K^+/Na^+ homeostasis in poplar species differing in salt tolerance. *Tree Physiol.* **29**, 1175–1186.

Tsugane, K., Kobayashi, K., Niwa, Y., Ohba, Y., Wada, K. and Kobayashi, H. (1999) A recessive Arabidopsis mutant that grows photoautotrophically under salt stress shows enhanced active oxygen detoxification. *Plant Cell*, **11**, 1195–1206.

Tuteja, N. (2007) Mechanisms of high salinity tolerance in plants. *Methods Enzymol.* **428**, 419–438.

Wang, W., Vinocur, B. and Altman, A. (2003) Plant responses to drought, salinity and extreme temperatures: towards genetic engineering for stress tolerance. *Planta*, **218**, 1–14.

Wang, A., Garcia, D., Zhang, H., Feng, K., Chaudhury, A., Berger, F., Peacock, W.J., Dennis, E.S. and Luo, M. (2010) The VQ motif protein IKU1 regulates endosperm growth and seed size in Arabidopsis. *Plant J.* **63**, 670–679.

Wei, W., Zhang, Y., Han, L., Guan, Z. and Chai, T. (2008) A novel WRKY transcriptional factor from *Thlaspi caerulescens* negatively regulates the osmotic stress tolerance of transgenic tobacco. *Plant Cell Rep.* **27**, 795–803.

Xie, Y.D., Li, W., Guo, D., Dong, J., Zhang, Q., Fu, Y., Ren, D., Peng, M. and Xia, Y. (2010) The Arabidopsis gene *SIGMA FACTOR-BINDING PROTEIN 1* plays a role in the salicylate- and jasmonate-mediated defence responses. *Plant, Cell Environ.* **33**, 828–839.

Xu, R.R., Qi, S.D., Lu, L.T., Chen, C.T., Wu, C.A. and Zheng, C.C. (2011) A DExD/H box RNA helicase is important for K^+ deprivation responses and tolerance in *Arabidopsis thaliana*. *FEBS J.* **278**, 2296–2306.

Zhang, H., Han, B., Wang, T., Chen, S., Li, H., Zhang, Y. and Dai, S. (2012) Mechanisms of plant salt response: insights from proteomics. *J. Proteome Res.* **11**, 49–67.

© 2013 The Authors

Zheng, Z., Qamar, S.A., Chen, Z. and Mengiste, T. (2006) Arabidopsis WRKY33 transcription factor is required for resistance to necrotrophic fungal pathogens. *Plant J.* **48**, 592–605.

Zhu, J.K. (2001) Plant salt tolerance. *Trends Plant Sci.* **6**, 66–71.

Zhu, J.K. (2002) Salt and drought stress signal transduction in plants. *Annu. Rev. Plant Biol.* **53**, 247–273.

Zhu, J.K. (2003) Regulation of ion homeostasis under salt stress. *Curr. Opin. Plant Biol.* **6**, 441–445.

Zou, C., Jiang, W. and Yu, D. (2010) Male gametophyte-specific WRKY34 transcription factor mediates cold sensitivity of mature pollen in Arabidopsis. *J. Exp. Bot.* **61**, 3901–3914.

© 2013 The Authors
The Plant Journal © 2013 John Wiley & Sons Ltd,